

# Spectral Measurement of Omnidirectional Light Distribution and Its Application to Image Rendering

*Shoji Tominaga and Norihiro Tanaka*

*Department of Engineering Informatics, Osaka Electro-Communication University  
Neyagawa, Osaka, Japan*

## Abstract

This paper proposes a method for estimating a set of spectral-power distributions of an omnidirectional light distribution from images taken by a camera aimed at a mirrored ball. First, we introduce some measuring systems that are designed for acquiring ambient light at any location in natural scenes. Second, a mapping algorithm is determined between coordinates on the ball and light rays in the world. Then we create images representing the omnidirectional light distribution. Third, the illuminant spectral-power distribution is recovered using the RGB image data and the calibrated reflectance data of the ball. Fourth, a CG image is created using the estimated omnidirectional illuminant distribution and a spectral-reflectance model for various objects. An experiment is conducted in our university gym.

## Introduction

Illuminant estimation in natural scenes includes the problem of estimating the spatial distribution of light sources by omnidirectional observations. Previous omnidirectional measuring systems used a mirrored ball, a fisheye lens, and a mirror with a hyperbolic surface. These measuring systems were originally developed for computer graphics (CG) and computer vision (CV).<sup>1,2</sup> Debevec<sup>1</sup> was the first to use a mirrored ball for acquiring an omnidirectional image that is a record of the illumination conditions in space. He did not calibrate the camera system. In a previous work<sup>3</sup> the authors calibrated an imaging system using a mirrored ball for acquiring an omnidirectional image.

However, all these works did not intend to infer illumination spectra, but intended to acquire the RGB color distribution of the ambient illumination at a particular point in space. In addition, the previous works had a certain inaccuracy in estimating the directional vectors of incident rays into the ball, so that the omnidirectional image was slightly distorted. It should be noted that the RGB information of ambient light has very limited applications in the fields of color engineering and image science. We can create realistic images of natural scenes that are rendered on

the spectral information of ambient light, but not on the RGB information.

The present paper proposes a method for estimating a set of spectral-power distributions of an omnidirectional light distribution from images taken by a camera aimed at a mirrored ball. The essential merits are (1) development of practical measuring systems using a mirrored ball, (2) estimation of precise illumination directions, (3) effective illuminant spectral estimation using a RGB camera, and (4) spectra-based image rendering.

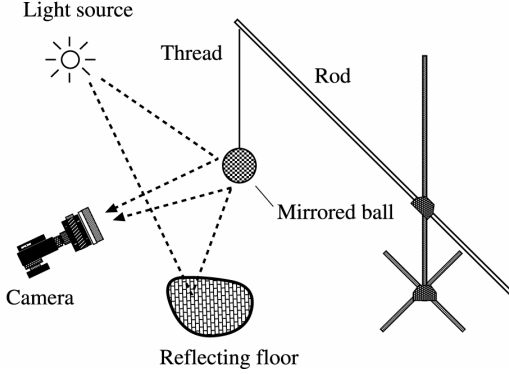
First, we introduce some measuring systems that are designed for acquiring ambient light at any location in natural scenes. Second, a mapping algorithm is determined between coordinates on a spherical ball and light rays in the world. Then we create images representing the omnidirectional light distribution. Third, the illuminant spectral-power distribution is recovered using the RGB image data and the calibrated reflectance data of the ball. Fourth, a CG image is created using the estimated omnidirectional illuminant distribution and a spectral-reflectance model for various objects.

## Measuring System

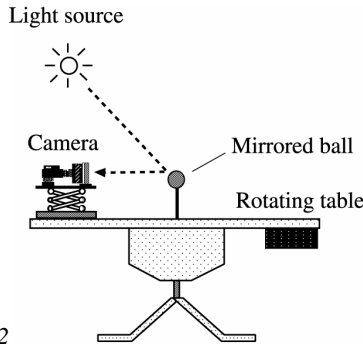
Figure 1 shows two types of measuring system using a mirrored ball that we have built for acquiring ambient light properties at any location in a natural scene. System 1 is a hanging-ball type where the ball is hung on a fish-line. This system is useful for collecting light rays from all surroundings by a single ball, including a reflecting floor as a light source. System 2 is the most precise type using a rotating table. The ball is mounted on the top of a short pole about which a table with a length of 80 cm is able to rotate. At the end of the table is a digital camera for imaging a particular view. The observable range is very wide, that is, the surrounding scenery of the ball for most directions is captured with a single image. The observable range is  $360^\circ - \psi$ , where  $\psi$  is the visual angle of the ball.

A Canon RGB digital camera, EOS D60, is used for estimating illuminant spectra. Each channel is represented by 12 bits, and images are sampled on a 2052x3088 pixels lattice. Figure 2 shows the spectral sensitivity functions in a

daylight mode. Note that the spectral bands are much broader than those of a multi-channel camera with more than three sensors (see Ref. [4]). Therefore, the RGB camera acquires spectral information less accurately than the multi-channel camera. Nonetheless, we had to use the RGB camera because of its much higher resolution and easier handling than the multi-channel camera.



System 1



System 2

Figure 1. Measuring systems using a mirrored ball.

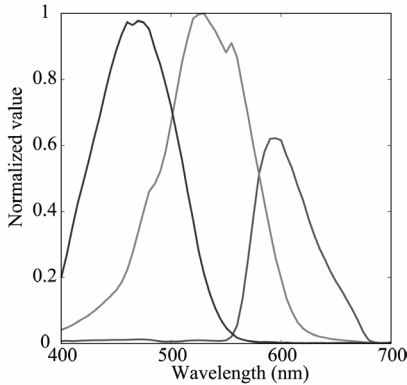


Figure 2. Spectral sensitivity functions of the camera.

## Estimation of Light-Directional Vectors

Figure 3 shows a geometric model for the measuring systems. A camera photographs the spherical mirror to obtain an omnidirectional radiance map around the location. In the figure,  $\mathbf{N}$  is the surface normal,  $\mathbf{L}$  is the light directional vector, and  $\mathbf{V}$  is the viewing vector. Moreover,  $\mathbf{V}_r$  is  $\mathbf{V}$  mirrored about  $\mathbf{N}$ . We assume that the ray beams from a light source are parallel. That is, the vector  $\mathbf{V}_r$  is the viewing vector in the direction of the light vector  $\mathbf{L}$  from the spherical center.

The illumination direction is estimated from an image projected on the mirrored ball. This computation requires camera parameters such as the focal length and the principal point. In a previous paper<sup>3</sup> we described a camera calibration method for measuring these parameters. Let  $\alpha$  and  $(x_0, y_0)$  be the generalized focal length of the lens and the coordinates of the optical axis on the image plane. If the image pixel is not square but rectangular, the generalized focal length is defined as  $(\alpha_x, \alpha_y)$  according to the  $x$  and  $y$  sizes.

The light directional vector is described as

$$\mathbf{L} = \mathbf{V}_r = \mathbf{V} - 2(\mathbf{N} \cdot \mathbf{V})\mathbf{N}. \quad (1)$$

In Eq.(1), the viewing vector  $\mathbf{V}$  and the surface normal  $\mathbf{N}$  are unknown, which are calculated using the spatial coordinates of the mirrored ball and the coordinates of the viewing direction on the image plane. Let  $(x, y)$  be the coordinates on the image plane.

First,  $\mathbf{V}$  is calculated as

$$\mathbf{V} = \frac{[(x-x_0)/\alpha_x, (y-y_0)/\alpha_y, 1.0]^t}{\left|[(x-x_0)/\alpha_x, (y-y_0)/\alpha_y, 1.0]^t\right|}. \quad (2)$$

Second, we calculate precisely the surface normal  $\mathbf{N}$  at  $(x, y)$ . For this computation, we determine the spatial coordinate vector  $\mathbf{M}$  of the ball center. Figure 4 shows the geometry for calculating the spatial position of the ball, where unit vectors  $\mathbf{C}$  and  $\mathbf{B}$  indicate a pointing vector from the camera center to the ball center and to any point at the ball's edge, respectively. Let  $\xi$  be an angle between  $\mathbf{C}$  and  $\mathbf{B}$ . Moreover, let  $d$  be the distance from the viewpoint to the ball center, and let  $r$  be the radius of the ball. Then  $d$  is calculated as  $d = r / \sin(\xi)$ . The intersection of  $\mathbf{V}$  and the ball is judged by using an index

$$t = (\mathbf{V} \cdot \mathbf{M}) - (\mathbf{M} \cdot \mathbf{M}) + r^2. \quad (3)$$

If  $t \geq 0$ ,  $\mathbf{V}$  intersects the ball. The distance from the viewpoint to the intersection point is calculated as

$$d_p = \min\left((\mathbf{V} \cdot \mathbf{M}) - \sqrt{t}, (\mathbf{V} \cdot \mathbf{M}) + \sqrt{t}\right). \quad (4)$$

Finally, the normal vector  $\mathbf{N}$  can be calculated as

$$\mathbf{N} = (d_p \mathbf{V} - \mathbf{M}) / \left\|d_p \mathbf{V} - \mathbf{M}\right\|. \quad (5)$$

The omnidirectional vectors are calculated by repeating the above procedure for all pixels of the ball image

$$\theta = \tan^{-1} \left( y_s / \sqrt{x_s^2 + z_s^2} \right), \phi = \tan^{-1} (x_s / z_s). \quad (6)$$

Calculation of the radiance values looking in all directions of  $(\theta, \phi)$  provides the omnidirectional image mapped on a sphere.

**Image Composition**

Let us consider the resolution of an image projected onto the mirrored ball. The central part of the image corresponding to the spherical center is sampled finely, but the outer part corresponding to the edge is sampled only roughly. In order to eliminate low resolution in the omnidirectional image, we acquire several images by observing the ball from different viewing angles and combine these images into one high-resolution image. This technique is effective especially for System 3.

Figure 6 shows a combination of three images observed with the rotational angle of 120-degree. Each image of the mirrored ball is transformed into one omnidirectional image represented in polar coordinates. Next, the central part corresponding to the range  $[-60 \leq \phi \leq 60]$  is cut out from the transformed omnidirectional image. Finally, these cut-out parts are combined into one image as shown in Figure 6. Lines and curves contained in the original images are very helpful in combining the images. We put the left image and right image with side by side. Then we combine two partial images into one image precisely so that lines, curves, and object edges in the left and right images meet smoothly without gaps at the joining line.

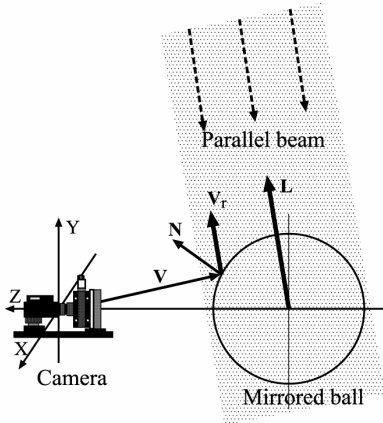


Figure 3. Geometric model of the observation.

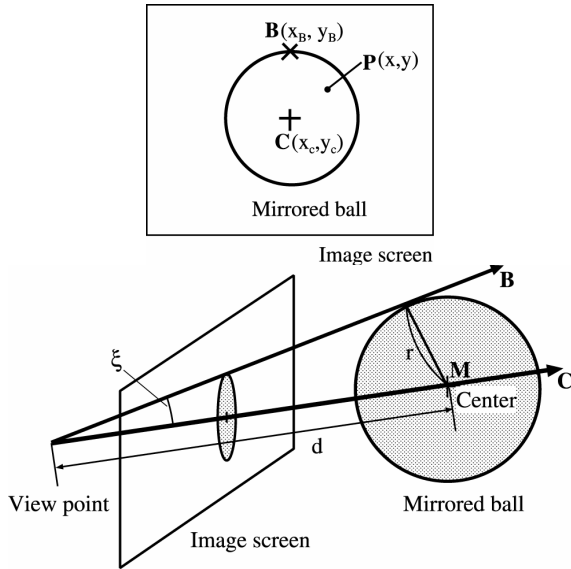


Figure 4. Calculation of the spatial position of the ball

**Creation of Omnidirectional image**

**Polar Coordinate Representation**

In order to represent the spatial distribution of ambient lighting, we create an omnidirectional image in a polar coordinate system. A set of the light vectors  $L$  points in all directions from the spherical center. Therefore, assuming a camera at the spherical center, we can produce an omnidirectional image observed at the center point. Let  $(x_s, y_s, z_s)$  be the rectangular coordinates on the spherical ball, and the axis  $z_s$  is assumed to be coincident with the optical axis  $Z$  as shown in Figure 5. The light vector is expressed in the polar coordinates  $(\theta, \phi)$  by transformation

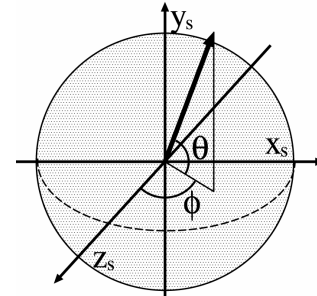


Figure 5. Polar coordinate system.

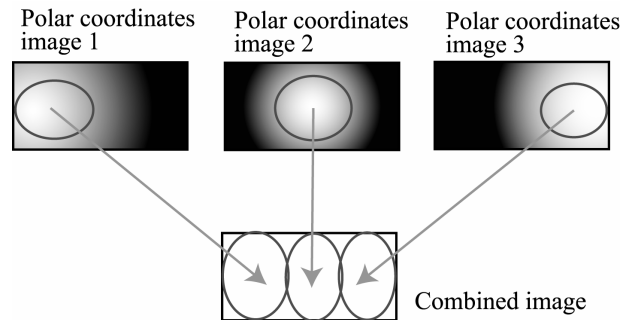


Figure 6. Combination of three images.

## Estimation of Illuminant Spectra

### Illuminant Recovery from RGB Camera Data

We use a finite-dimensional linear model for describing illuminants by a small number of unknown parameters. As a result, the linear model with *three* parameters makes it possible to recover the spectral functions from the RGB camera data. We assume that the illuminant spectrum  $E(\lambda)$  can be expressed as a linear combination of *three* basis functions as

$$E(\lambda) = \sum_{i=1}^3 \varepsilon_i E_i(\lambda), \quad (7)$$

where  $\{E_i(\lambda), i=1, 2, 3\}$  is a statistically determined set of basis functions, and  $\{\varepsilon_i\}$  is a set of scalar weights. A set of the measured spectra of nine light sources was used for determining the illuminant basis functions. Figure 7 shows the basis functions used in this study, which were obtained as the first three principal components of the set of illuminant spectra.

The camera output at spatial location  $x$  is described as

$$\begin{bmatrix} R(x) \\ G(x) \\ B(x) \end{bmatrix} = \int_{400}^{700} S(x, \lambda) E(\lambda) \begin{bmatrix} r(x) \\ g(x) \\ b(x) \end{bmatrix} d\lambda, \quad (8)$$

where  $S(x, \lambda)$  is the surface-spectral reflectance function of the mirrored ball, and  $\{r(\lambda), g(\lambda), b(\lambda)\}$  are the spectral sensitivity functions of the camera. The surface-spectral reflectance function was determined by the Fresnel reflectance for polished metal as

$$S(x, \lambda) = F(\theta_i, n(\lambda), k(\lambda)) / \cos(\theta_i), \quad (9)$$

where  $\theta_i$  is the angle of incidence,  $k(\lambda)$  is the absorption coefficient,  $n(\lambda)$  is the index of refraction.

The illuminant weight vector is determined in the form

$$\boldsymbol{\varepsilon} = \boldsymbol{\Lambda}_{S(x)}^{-1} \boldsymbol{\rho}(x), \quad (10)$$

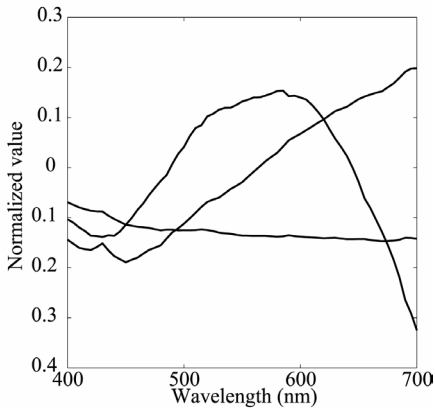


Figure 7. Basis functions for illuminant spectra.

where  $\boldsymbol{\rho}(x)$  is the camera output vector defined by  $\boldsymbol{\rho}(x) = [R(x), G(x), B(x)]^T$  and  $\boldsymbol{\Lambda}_{S(x)}$  is a  $3 \times 3$  matrix with the elements  $[\int E_i(\lambda) S(\lambda) r(\lambda) d\lambda \dots]$ . Finally, the estimated curve of the illuminant  $E(\lambda)$  is obtained by substituting the estimate of  $\boldsymbol{\varepsilon}$  into Eq.(7).

### Reflectance of the Mirrored Ball

Our mirror ball is made from stainless steel (SUS304). The SUS304 steel is an alloy of iron (74%), chrome(18%), and nickel (8%). Generally, the reflectance of a segregation alloy is described as a weighted mean of the contained materials. Consequently, the spectral reflectance  $S(x, \lambda)$  can be described as a function of the incident angle of illumination as follows:

$$\begin{aligned} S(x, \lambda) = & 0.74 \cdot F(n_{Fe}(\lambda), k_{Fe}(\lambda), \theta_i) \\ & + 0.18 \cdot F(n_{Cr}(\lambda), k_{Cr}(\lambda), \theta_i) + 0.08 \cdot F(n_{Ni}(\lambda), k_{Ni}(\lambda), \theta_i) \end{aligned} \quad (11)$$

where  $\theta_i$  is the incident angle that is calculated from  $\theta_i = \cos^{-1}(\mathbf{N} \cdot \mathbf{L})$ . The optical constants  $n_{Fe}(\lambda), k_{Fe}(\lambda), n_{Cr}(\lambda), k_{Cr}(\lambda), n_{Ni}(\lambda), k_{Ni}(\lambda)$  are the reflective indices and absorption coefficients for iron, chrome, and nickel, respectively.

## Image Rendering

The omnidirectional spectral distribution as estimated above can be used as an ambient light source for rendering synthetic objects into real scenes. Spectra-based image rendering using illuminant spectral-power distribution has the advantage that the interaction between light rays and object surfaces is calculated with physical accuracy, and the color appearance of the objects in a natural scene is realized in a color image based on human color perception.

A realistic image of virtual objects existing in a real lighting environment is rendered using the ray tracing algorithm. We use the Torrance-Sparrow model for describing spectral reflection on any object surface. The spectral radiance  $Y(\lambda)$  is then represented as

$$\begin{aligned} Y(x, \lambda) = & \int_{\Omega} [\alpha \cos(\theta_i) S(x, \lambda) E(\lambda) \\ & + \beta \frac{D(\varphi, \gamma) F(\theta_q, n(\lambda), k(\lambda)) G(\mathbf{N}, \mathbf{V}, \mathbf{L})}{\cos(\theta_i)} E(\lambda)] d\Omega, \\ & + \beta' (\text{mirrored reflection term}) \end{aligned} \quad (12)$$

where the first and second terms in the integral of the right hand side corresponds to two components of diffuse reflection and specular reflection, respectively. The second term of the right hand side is a perfect mirror component. The constants  $\alpha, \beta$  and  $\beta'$  are the weights of the respective components. Moreover,  $\theta_i$  is the incident angle,  $\theta_r$  is the viewing angle,  $\varphi$  is the angle between the global

surface normal and micro-facet normals, and  $\theta_0$  is the angle of incidence to a micro-facet. The specular reflection component consists of several terms,  $D$ : function providing the index of surface roughness defined as  $\exp\{-\ln(2)\varphi^2/\gamma^2\}$ , where  $\gamma$  is constant,  $G$ : geometrical attenuation factor, and  $F$ : Fresnel spectral reflectance of the material consisting of an object surface.

## Experimental Results

We acquired spectral-power distributions of an omnidirectional light source in our university gym. Figure 8 shows the real view of System 2 used in this experiment. We captured three other images of the ball from the rotational angles of  $\pm 120$ -degree. These three images were transformed to polar coordinates and combined into a single omnidirectional image. Figure 9 shows the resultant omnidirectional image.

The illuminant spectral-power distribution was estimated from the RGB camera data at each pixel point. Figure 10 shows the estimation results of illuminant spectra for area 1 in Figure 9, which corresponds to the ceiling lamp. The blue curve indicates the estimated spectrum of the incandescent light source, and the red curve is the direct measurement by using a spectro-radiometer. Figure 11 shows the estimation results for area 2, corresponding to the outer daylight source through a side window. The estimated spectral curves have some variations at pixel point. The comparison between the estimates and measurements suggests the reliability of the proposed method. It should be noted that we are able to obtain these results by simply using an off-the-shelf RGB digital camera.

Image rendering for augmented reality was executed using the estimated omnidirectional illuminants. Three metallic objects with different materials of gold, silver, and copper are the virtual objects in the real scene of the gym. These objects are illuminated with the real ambient light sources. Moreover, we assumed that the original window glasses were replaced with stained glasses of red, yellow, and green. The spectral transmittance data of these stained glasses were obtained from direct measurements of the real colored glasses. The spectral radiance reflected from the virtual objects was calculated using the model of Eq.(13). Then ray-tracing image rendering was executed based on spectral computation over the visible range of 400-700 nm in 5 nm increments. The spectral image was converted into an image expressed in the CIE-XYZ tristimulus values. Finally the image was displayed on a calibrated monitor.

Figure 12 demonstrates the resulting image rendered under the above conditions. The objects are a small ball of silver, a large ball of copper, and a gold pedestal. These object surfaces are illuminated with the transmitted daylight sources through the stained glasses and the real incandescent sources from the ceiling. Figure 13 shows the color shifts for gold, silver, and copper on the xy-chromaticity diagram between the original spectral-based computation and the RGB-based computation at 460, 530, and 600 (nm) channels. The light source is assumed as D65. This suggests

the importance of the spectra-based image rendering method.



Figure 8. Real view of System 2 in the gym.

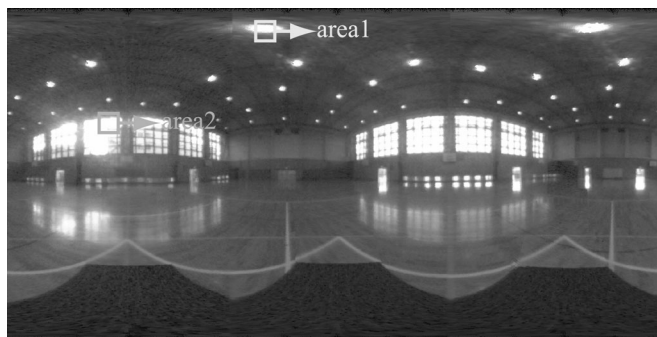


Figure 9. Combined omnidirectional image of the gym.

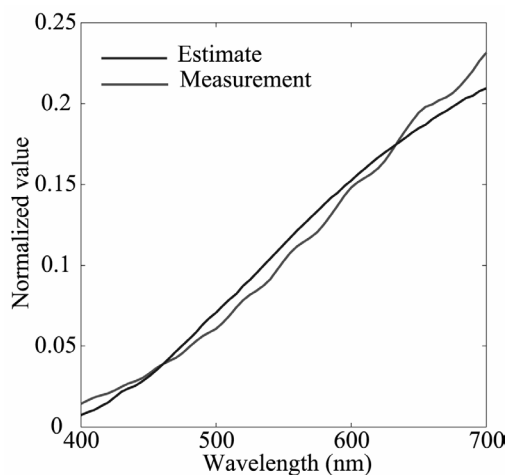


Figure 10. Estimation results for area 1.

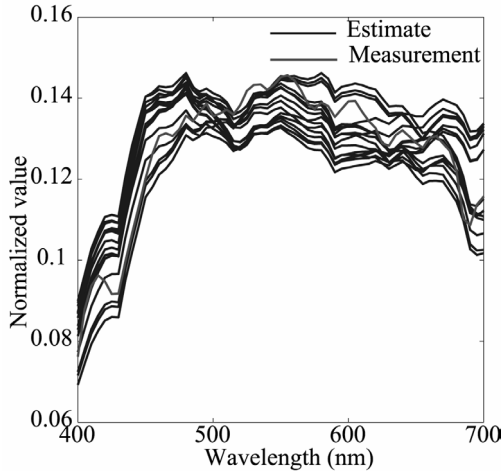


Figure 11. Estimation results for area 2.



Figure 12. Spectra-based image rendering.

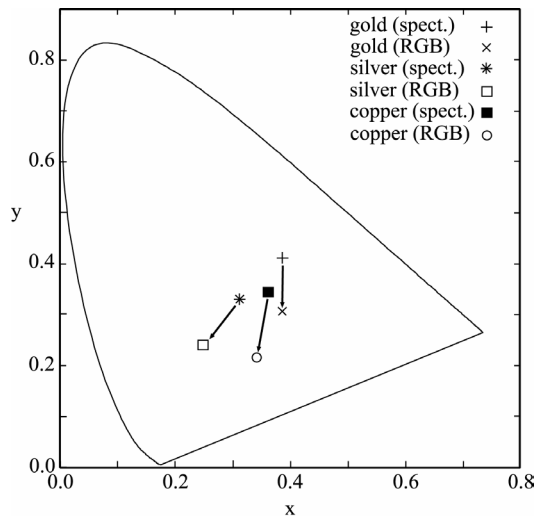


Figure 13. RGB-based image rendering.

## Conclusion

This paper has described a method for estimating a set of spectral-power distributions of an omnidirectional light distribution from images taken by a camera aimed at a mirrored ball. The essential merits are (1) development of practical measuring systems using a mirrored ball, (2) estimation of precise illumination directions, (3) effective estimation of illuminant spectra by using a normal RGB camera, and (4) spectra-based image rendering. We introduced two measuring systems that were designed for acquiring ambient light at any location in natural scenes. In an experiment, we acquired spectral-power distributions of an omnidirectional light source in our university gym, and executed image rendering by using the estimate source.

## References

1. P. E. Debevec: Rendering synthetic objects into real scenes, *Proc. SIGGRAPH 98*, pp.189-198, 1998.
2. S. K. Nayar: Computational imaging, *Proc. The 10th Color Imaging Conf.: Color Science and Engineering, Systems, and Applications*, p.6, 2002.
3. S. Tominaga and N. Tanaka: Measurement of omnidirectional light distribution by a mirrored ball, *Proc. The Ninth Color Imaging Conf.: Color Science, Systems, and Applications*, pp.22-26, 2001.
4. S. Tominaga: Spectral imaging by a multi-channel camera, *Journal of Electronic Imaging*, Vol. 8, No. 4, pp. 332-341, 1999.

## Biography

**Shoji Tominaga** received the B.E., M.S., and Ph.D. degrees in electrical engineering from Osaka University, Toyonaka, Osaka, Japan, in 1970, 1972, and 1975, respectively. Since 1976, he has been with Osaka Electro-Communication University, Neyagawa, Osaka, where he is currently a Professor with the Department of Engineering Informatics, and a Dean of the Faculty of information Science and Arts. His research interests include computer graphics, color image analysis, reflection modeling, and color vision. He is a senior member of IEEE and a member of OSA, IS&T, SID, SPIE, and ACM.